

MSC WORLD USERS' CONFERENCE  
Arlington, Virginia, May 1993

**"RESPONSE OF PROTECTIVE STRUCTURES TO  
INTERNAL EXPLOSIONS WITH BLAST VENTING"**

Y. Kivity \*, C. Florie and H. Lenselink  
The MacNeal-Schwendler Company B.V.  
Gouda, The Netherlands

**Abstract**

This paper presents a computational study of the response of generic protective structures to internal blast waves from high explosive charges. The computations are carried out with the three-dimensional program MSC/DYTRAN, with explicit treatment of the fluid-structure interactions inherent to the problem. The modelled generic structures include frangible panels for blast venting and internal partitions for blast wave deflection. The structural description includes both a thin shell approach for thin walled containers and a solid finite element representation for concrete type structures. The flow of the detonation products and the ambient air is described employing an Arbitrary-Lagrange-Euler (ALE) approach. This approach also allows internal partitions to be attached to the ALE mesh without degrading the computational efficiency.

---

\*) on leave of absence from RAFAEL Ballistics Center, Haifa, Israel.

## 1. INTRODUCTION

Determination of the response of a structure subjected to an internal explosion requires the combination of two disciplines: structural dynamics and fluid dynamics. Both disciplines have to be applied in regimes of considerable complexity due to the nature of the problem. Consider first the structural dynamics. Due to the intense load, large deformations are to be expected, with corresponding nonlinear material behavior, including possible fracture. The fluid dynamics problem poses comparable difficulties: as the structure is loaded significant displacements may occur, and thus the flow boundaries are dynamically modified (in contrast with classical fluid dynamics with fixed boundaries). Furthermore, the flow field contains extreme discontinuities at the start (orders of magnitude in terms of pressure and density), creating strong shock waves which are subsequently diffracted by obstacles and/or reflected from the structure walls. In view of these complexities, the dynamic response of structures to loads which originate from the coupled motion of an adjacent fluid are now commonly designated as "Fluid-Structure Interactions".

The design of protective structures in the past relied heavily on semi-empirical and experimental data collected by workers in the field. The main source of information was the American TM5-1300 manual [1]. The information in this manual gave general information on the design, but the lack of specific data for a particular application may result in over-conservative designs.

For vented structures, with or without frangible panels, Reference [2] furnishes experimental data obtained by the Naval Civil Engineering Laboratory (NCEL) at Port Hueneme, CA. Some simplified mathematical models for the effects of frangible panels may be found in [3]. A more recent study [4] combined theoretical results and experimental data and reduced them to a single "working curve" using similarity methods.

The use of detailed flow calculations for determining the loads resulting from internal explosions in rigid structures was presented in recent seminars of the DoD Explosives Safety Board [5-9]. These studies were limited to rigid structures so that the full fluid-structure interactions were not taken into account. This limitation stemmed mainly from the lack of appropriate codes and to a lesser degree from the limited capabilities of computers at that time.

The new generation of cost-efficient computers gave a renewed impetus to the development of numerical schemes for solving multi-dimensional shocked flows. These schemes were implemented in large scale computer codes (commonly called hydrocodes) which are intended for treating a variety of problems with sufficient generality in terms of the geometry definition, material models, and application of initial and boundary conditions. Using a hydrocode, the complex flow fields created by internal explosions may be treated. Such flow fields may include wave reflections and diffraction by solid obstacles, and blast wave venting through openings. These capabilities enable the protective structure designer to optimize the structure and thus avoid a costly over-conservative design.

In the present work we employ the MSC/DYTRAN program for studying the response of a generic structure to internal explosions. This program includes several processors which combine to give a powerful tool for treating all aspects of protective structure design. Some theoretical background of the code is given in [10]. An overview of the cases modelled in this study is given in the next section. Section 3 describes the representation of the high explosive charge. The results of the calculations are discussed in Section 4, and conclusions are presented in Section 5.

## **2. OVERVIEW OF MODELLED CASES**

A total of six cases were calculated. They may be divided into three categories:

1. Rigid Structures with venting ports or doors (Cases 1, 2 and 3).
2. Thick-walled structures with venting ports or doors (Cases 4 and 5).
3. Thin-walled containers (Case 6).

The rigid and thick-walled structures are variations of the same generic structure, shown in Figure 1. The thin walled container is a right-circular cylinder, closed by flat ends, see Figure 2.

The generic structure consisted of a cubicle 1 m x 1 m x 1 m, with an opening of 0.7 m x 0.7 m at one side. The blast wave is generated by a high explosive charge of 1 kg TNT, placed along the double symmetry line which divides the cubicle into four symmetric parts. Figure 3 shows the computational mesh for one symmetrical quarter. The structure is embedded in a sufficiently large Euler mesh to allow the calculation of the flow field generated outside the structure by the blast wave after it vents. The overall size of the computational mesh (for the "quarter problem") is 0.75 m x 0.75 m x 1.5 m.

The computational mesh for the problem consisted of 6750 Euler elements (cubes with a side of 0.05 m). In the thick-walled structures there were additional Lagrange elements for representing the wall (about 550). Cases 1 and 4-6 were computed for a physical time of 2.85 ms, whereas Cases 2 and 3 were computed to 6 ms. A typical run took less than 30 minutes on a CRAY-YMP/EL.

The thin-walled cylindrical container, with a diameter of 0.9 m and an overall length of 7.2 m, was stiffened via rings and closed by flat caps. The charge was placed at the middle of the cross-section of the cylinder so that only a symmetric quarter of the problem needed to be considered in the modelling. The computational model (Figure 9) involved about 3500 Euler elements for the gas, and about 400 elements for the shell. The calculation was carried out to a physical time of about 10 ms in order to include the blast wave reflections from the closed end. The calculation took about 20 minutes on a CRAY-YMP/EL. A similar container was tested and analyzed by the Wright Laboratory of Wright-Patterson Air Force Base [11].

### **3. REPRESENTATION OF THE EXPLOSIVE**

When modelling the detailed interaction of a high explosive with an adjacent material, it is important to represent the correct shape of the explosive charge and to simulate adequately the detonation process. In blast wave modelling, however, the exact shape of the explosive and the details of the detonation process have a small effect on the blast wave characteristics at large distances from the explosive.

To simplify the present calculations, we represent the explosive as a sphere of dense and hot gas with the correct mass and energy of the explosive charge. The gas is assumed ideal so that the only material property that remains to be determined is the ratio of specific heats,  $\gamma$ . A typical value of  $\gamma$  for the detonation products at low pressure would be about 1.3. In order to simplify the calculations further, we use the same  $\gamma$  value as for air, i.e. 1.4. In this way the Euler flow calculation involves a single material. Based on previous experience, this simplification only affects the blast wave impulse by about 5%, which is of the same order of magnitude of the uncertainty in the explosive energy.

Typical values for a high explosive are a density of  $1600 \text{ kg/m}^3$  and a detonation energy of  $4.5 \text{ MJ/kg}$ . The initial high density makes the volume of the initial conditions region very small in terms of the number of Euler elements. For a  $1 \text{ kg}$  charge, the volume would be  $0.625 \times 10^{-3} \text{ m}^3$  or a sphere with a radius of  $0.053 \text{ m}$ . Since we are using a mesh with an element size of  $0.05 \text{ m}$ , the charge would occupy just one element, resulting in excessive diffusion due to the large pressure and density discontinuity. To circumvent this problem, a larger volume is used for defining the initial conditions with a corresponding lower density. The effect of lower initial charge density was studied in [6]. It was found that the effect of an 8 fold increase of the density (from  $25 \text{ kg/m}^3$  to  $200 \text{ kg/m}^3$ ) amounted to less than 5% difference in the impulse on the walls. In the current calculations, an initial density of  $238 \text{ kg/m}^3$  is used (or a sphere radius of  $0.1 \text{ m}$ ).

#### **4. RESULTS**

The results of the calculations will be presented and discussed in accordance with the three categories mentioned in the previous section.

##### **Rigid Structures**

The rigid walls of the structure are represented by an impervious boundary in the Euler computational mesh, which outlines the geometrical shape of the desired wall. See Figure 3. The flow boundary is constructed from element faces which are assigned a rigid wall boundary condition by preventing any transport across them. In this way internal rigid walls may be represented with a minimal effort. This requires, however, that the Euler computational mesh is aligned with the walls of the structure.

The rigid structure has an opening of  $0.7 \text{ m} \times 0.7 \text{ m}$  (or  $0.35 \text{ m} \times 0.35 \text{ m}$ , in the “quarter” model), which corresponds to a non-dimensional vent area  $A/V^{2/3} = 0.49$ . This opening is covered by a door, represented by a single Lagrange element with a face slightly larger than the opening. This element is given elastic and strength properties sufficiently high such that it will remain practically rigid under the blast loading. The mass per unit area of the door is  $10 \text{ kg/m}^2$ .

Three cases were calculated with this basic configuration:

#### CASE 1:

In this case the doors are assumed to be hinged to the rigid walls as indicated in Figure 3. Under the action of the blast wave, the door swings open at a rate governed by its moment of inertia and the blast load. As the door rotates, an increasing area becomes available for blast venting which reduces the average pressure inside the chamber. Figure 4 shows the velocity vector at selected times for a cross-section containing the charge and parallel to the floor ("top view"). It is evident that significant venting occurs after  $t = 1.3$  ms. Note that the first reflection of the wave from the walls is almost symmetrical with respect to the symmetry plane containing the charge center and parallel to the door. This is a result of the fact that the door does not move significantly during this first reflection due to inertial resistance.

#### CASES 2 & 3:

These two cases were designed to bring out the effect of venting. In both cases the door is not hinged but is attached to the walls by non-linear structural members. In Case 2 there is an opening in the ceiling, which provides venting of the blast wave and thus reduces the overall internal load. Case 3 does not have such an opening. As a result, the door is blown off in the non-vented case due to failure of the attachment structure. In contrast, the door in the vented structure remains attached as the blast impulse is not sufficient to cause failure of the attachment.

The attachment structure in these calculations was equivalent to a steel shell having a thickness of 0.9 mm, a yield strength of 0.4 GPa and a failure strain of 0.003. The opening for the full structure was 0.4 m x 0.6 m, or a nondimensional area  $A/\sqrt{2/3} = 0.24$ . The flow field is depicted in Figure 5 for Case 2 and in Figure 6 for Case 3. These figures show a cross-section containing the charge and normal to the floor ("side view").

## **Thick-Walled Structures**

### CASE 4:

In this case, the cubicle has deformable walls. The walls are represented by solid Lagrange elements. For the coupling between the wall motion and the fluid elements, the Arbitrary-Lagrangian-Eulerian (ALE) method is employed. This results in a very efficient calculation, since the computation intensive general coupling algorithm is not needed.

The wall material is assumed elastic-perfectly-plastic, with a Von-Mises yield criterion. The material parameters were chosen to represent a concrete wall, heavily reinforced by steel bars and steel liners. Such walls are commonly used for protective structures. The wall thickness was taken as 0.05 m in proportion to the cubicle dimensions which may represent a scaled down protective structure. Assuming a scaling factor of 4, the "real" structure would be a 4m x 4m x 4m building, with a 0.2 m concrete wall, having about 1 % steel reinforcement and an 8 mm steel liner. Such a wall would withstand significant strains before failure. The corresponding scaled-up charge weight would be 64 kg.

Figure 7a show the flow field at selected times together with the deformed shape of the wall ("side view").

### CASE 5:

This case is similar to Case 4, except that a light weight partition was introduced in the mid cross-section, occupying about 40% of the cross-section area. The partition is attached to the ALE grid points, so that the calculation can still proceed with the same efficiency as before.

The partition modifies the flow field by forcing the blast wave to diffract over it. The charge weight was halved, to keep the ratio of the charge to the volume of the partitioned chamber at the level of the previous cases. The capability of introducing light weight partitions without the penalty of increased modelling complexity can be very useful for representing fire protection partitions.

The flow field for this case is depicted in Figure 8, where velocity vectors are shown together with the deformed walls and the displaced partition ("side view").

### **Thin-Walled Structures**

#### CASE 6:

The response of thin-walled structures to internal explosions has received much attention recently as a result of an FAA program to harden commercial aircrafts against the effects of terrorist explosive charges. Within the framework of this FAA program, tests involving cylindrical containers have been carried out at Wright Patterson AFB. The calculation presented here constitutes a coarse mesh simulation of one of these tests. The details of the analysis and test were reported in [11].

The computational mesh for this case is shown in Figure 9. The Euler elements are not shown, except for the inner core near the axis of symmetry. The charge occupied the eight elements adjacent to the symmetry cross-section.

The evolution of the blast wave is shown in Figures 10-11, in a sequence of velocity vector plots superimposed on pressure contours. At  $t = 0.1$  ms the main blast wave has already formed. A deviation from spherical symmetry is observed, which is attributed to the fact that the charge is not spherical - it is very close to a cylinder with a height to diameter ratio of about 2. At  $t = 0.2$  ms the main shock front hits the wall, and at the same time a low pressure core is generated at the center of the explosion, which subsequently ( $t = 0.3$  ms) reverses the flow direction. This trend continues also at  $t = 0.4$  ms, while the high pressure region created at the wall continues to travel axially. The flow reversal near the axis combines with the inward flow created by the reflection at the wall, and as a result a high pressure core is formed again at the origin ( $t = 0.6$  ms). This high pressure core progresses axially, and will eventually overtake the main wave front and form an almost uniform shock front over the cross-section.

The response of the shell to the blast is shown in Figure 12 via effective plastic strain contours. A ring of high strain is located near the charge cross-section. A higher strain, however, is found at the rim of the circular end, obviously resulting from severe bending caused by the loading of the axially progressing wave.



## **5. CONCLUDING REMARKS**

The six calculations presented in this paper demonstrate the usefulness of a 3D coupled fluid-structure interaction code as a practical tool in the area of protective structures and explosive containment.

The MSC/DYTRAN approach makes it possible to take into account complex geometries, blast wave reflection and venting, fluid-structure interaction and highly nonlinear material properties. The combination of these capabilities into one code provides the protective structures designer with a powerful tool for optimizing designs instead of relying on semi-empirical data. Considering the new generation of cost-efficient computers, such 3D calculations are not only feasible but also economically beneficial, since they can lead to optimized structures and thus avoid costly and over-conservative design practices.

## **Acknowledgement**

The authors wish to thank Mr. Mike Howe for editing the manuscript. His assistance in generating the superimposed plots is appreciated.

## **References:**

- [1] "Structures to Resist the Effects of Accidental Explosions".  
Army TM5-1300, Dept. of the Army, Navy and Air Force; Washington D.C., June 1969.
- [2] (a) Keenan, W.A. and Tancreto, J.E.: "Blast Environment from Fully and Partially Vented Explosions in Cubicles".  
Tech. Rep. 51-027, NCEL, Port-Hueneme, CA (1974).  
(b) Keenan W.A. and Tancreto J.E.: "Design Criteria for Frangible Covers in Ordnance Facilities".  
Proceedings of the 20th DoD Explosives Safety Seminar, pp. 333-362, Norfolk 1982.  
(c) Tancreto J.E. and Helseth E.S.: "Effect of Frangible Panels on Internal Gas Pressures".  
Proceedings of the 21th DoD Explosives Safety Seminar, pp. 365-394, Houston 1984.
- [3] Kulesz, J.J. and Friesenhahn, G.J.: "Explosion Venting in Buildings".  
Proceedings of the 19th Explosive Safety Seminar, pp. 413-428, Los Angeles 1980.

- [4] Anderson, C.E. et al: "Quasi-Static Pressure, Duration and Impulse for Explosions in Structures".  
Int. J. Mech. Sci., Vol. 25, No. 6, pp. 455-464, 1983.
- [5] Gregory, F.H.: "Analysis of the Loading and Response of a Suppressive Shield when Subjected to an Internal Explosion".  
Proceedings of the 17th DoD Explosives Safety Seminar, pp. 743-760, Denver 1976.
- [6] Kivity, Y. and Feller, S.: "Blast Venting from a Cubicle".  
Proceedings of the 22nd DoD Explosives Safety Seminar, Anaheim, CA., August 1986.
- [7] Kivity, Y. and Kalkstein, A.: "Blast Wave Penetration into Cubicles".  
Proceedings of the 23rd DoD Explosives Safety Seminar, 9-11 August 1988, Atlanta, GA.
- [8] Kivity, Y. and Palan, D.: "The Internal Blast Wave Produced in a Closed Range by a 155 mm Howitzer Gun".  
Proceedings of the 24th DoD Explosives Safety Seminar, 28-30 August 1990, St. Louis, Missouri.
- [9] Kivity, Y.: "The Reflected Impulse on a Curved Wall Produced by a Spherical Explosion in Air".  
25th DoD Explosives Safety Seminar, Anaheim, CA., August 1992.
- [10] Kivity, Y., Florie, C. and Lenselink, H.:  
"The Plastic Response of a Cylindrical Shell Subjected to an Internal Blast Wave with a Finite Width Shock Front".  
Proceedings of the 33<sup>rd</sup> Israel Annual Conference on Aviation and Astronautics, Israel 24-25 February 1993.
- [11] Ewing, M.S., Kivity, Y. and Lenselink, H.:  
"Internal Blast Response of Ring-Reinforced Thin Walled, Right Circular Cylinder: Analysis and Test".  
Proceedings of the FAA Aircraft Hardening and Survivability Symposium, Atlantic City, New Jersey, August 11-13, 1992.

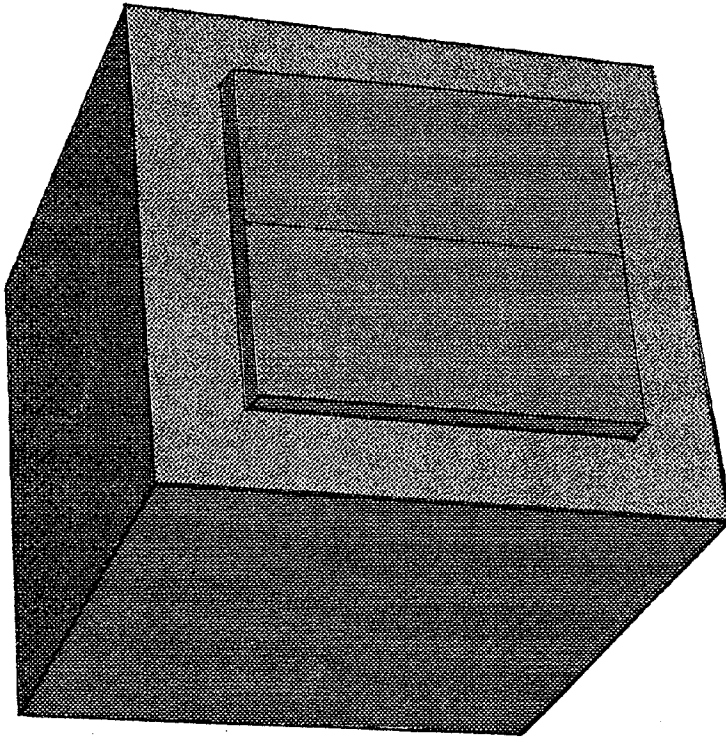


FIGURE 1 : GENERIC PROTECTIVE STRUCTURE (SCHEMATIC)

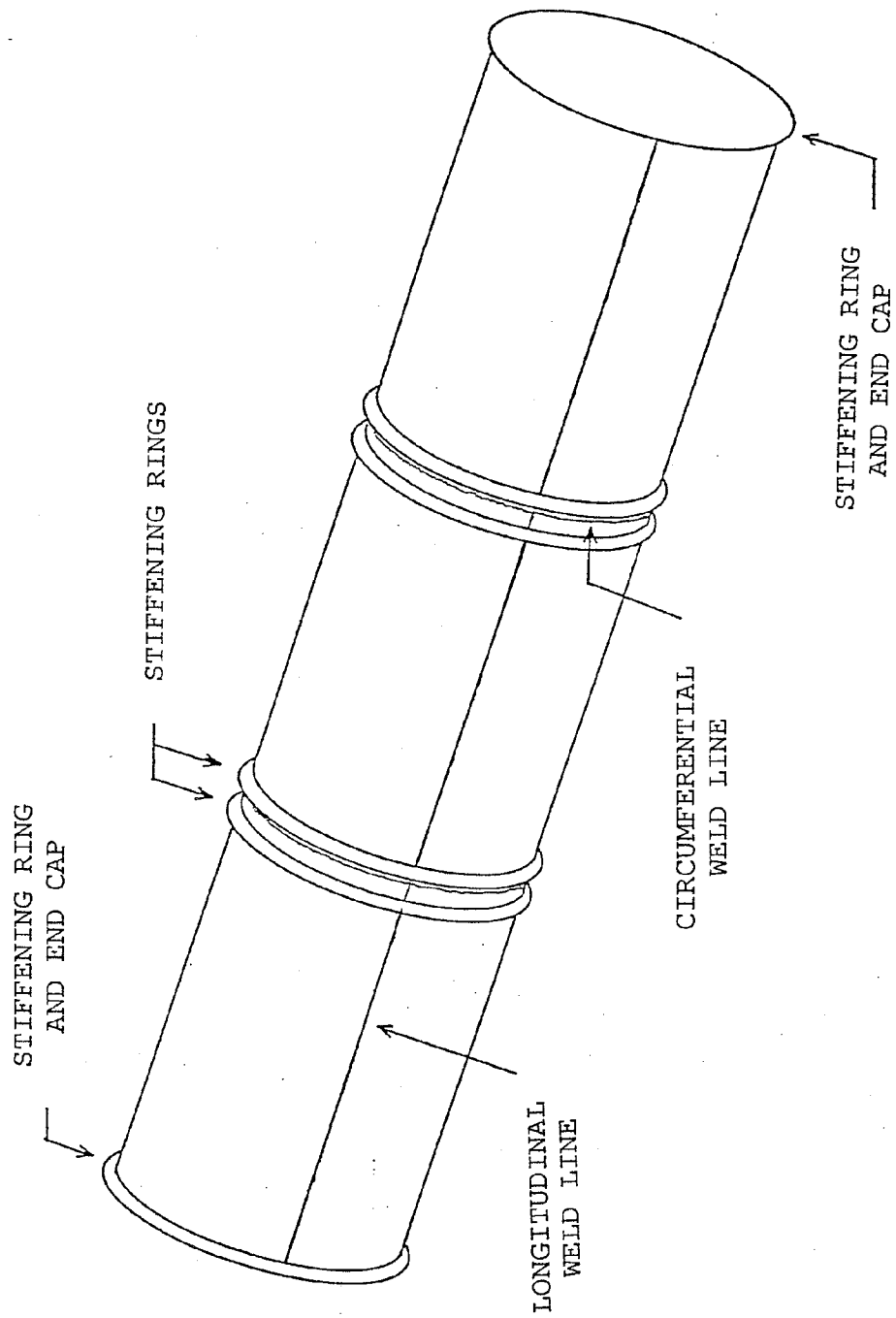


FIGURE 2 : CYLINDRICAL CONTAINER

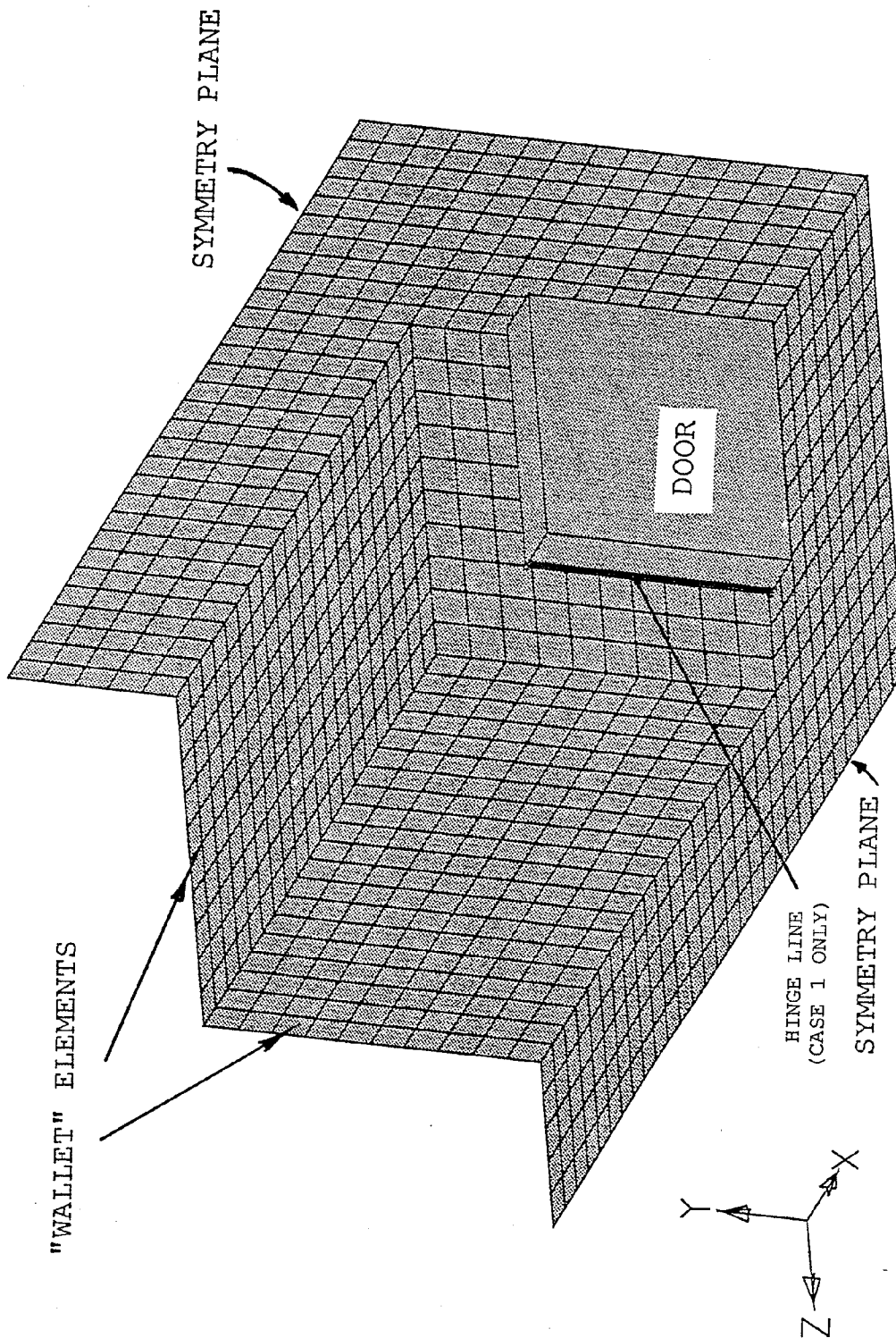


FIGURE 3 : COMPUTATIONAL MESH FOR THE GENERIC STRUCTURE  
(EULER HEXA ELEMENTS NOT SHOWN)

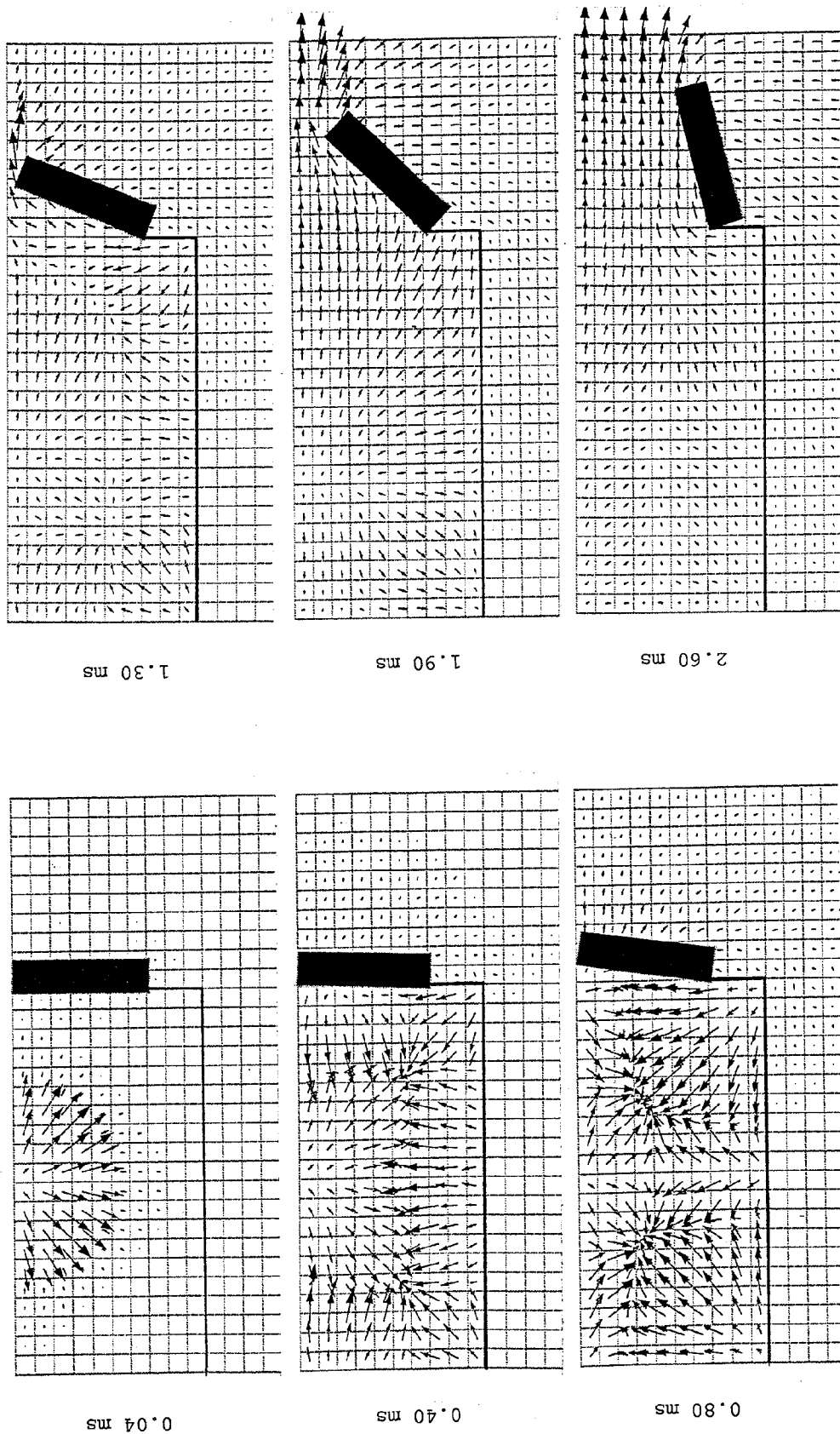


FIGURE 4 : VELOCITY VECTOR PLOTS AT SELECTED TIMES (CASE 1)

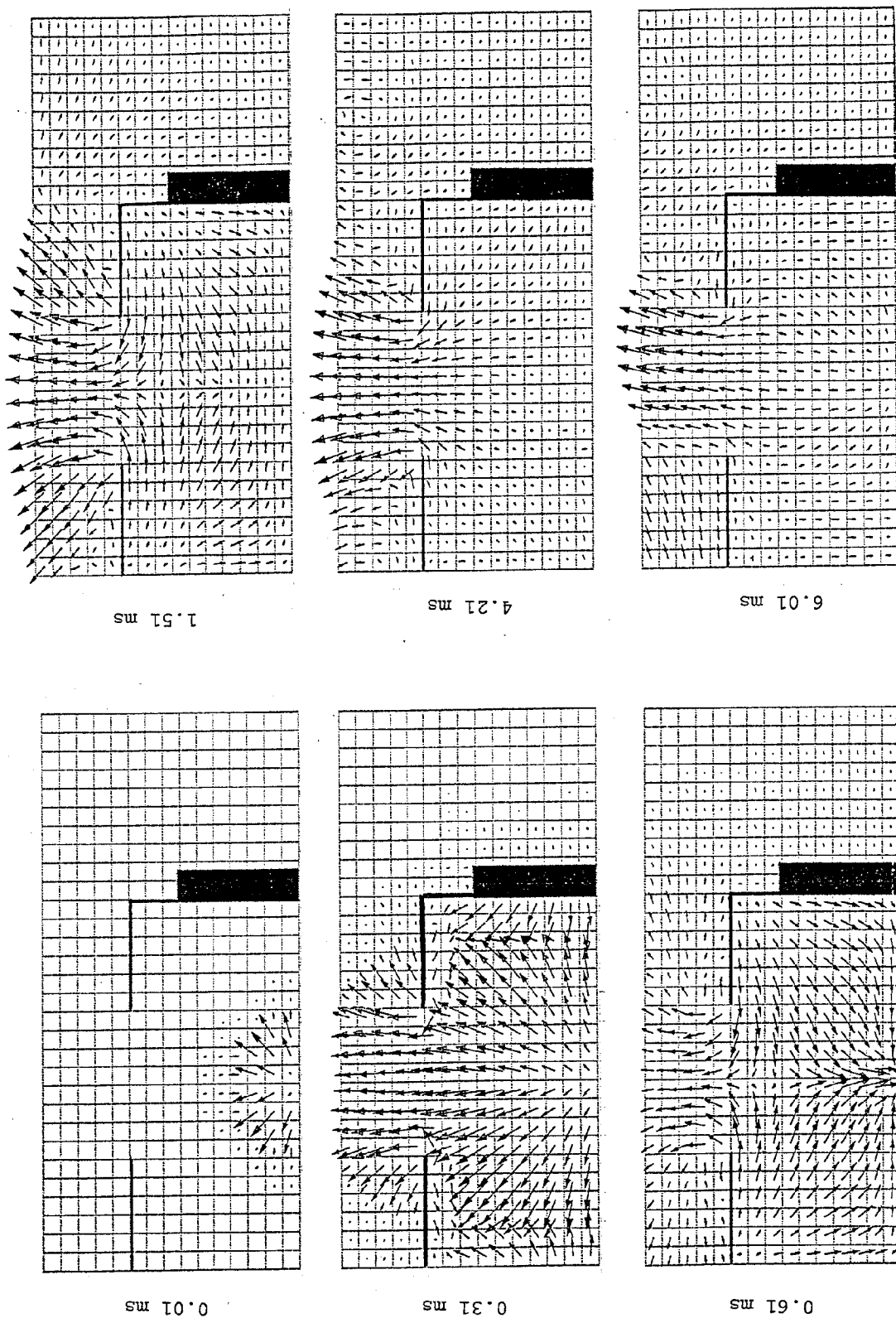


FIGURE 5 : VELOCITY VECTOR PLOTS AT SELECTED TIMES (CASE 2)

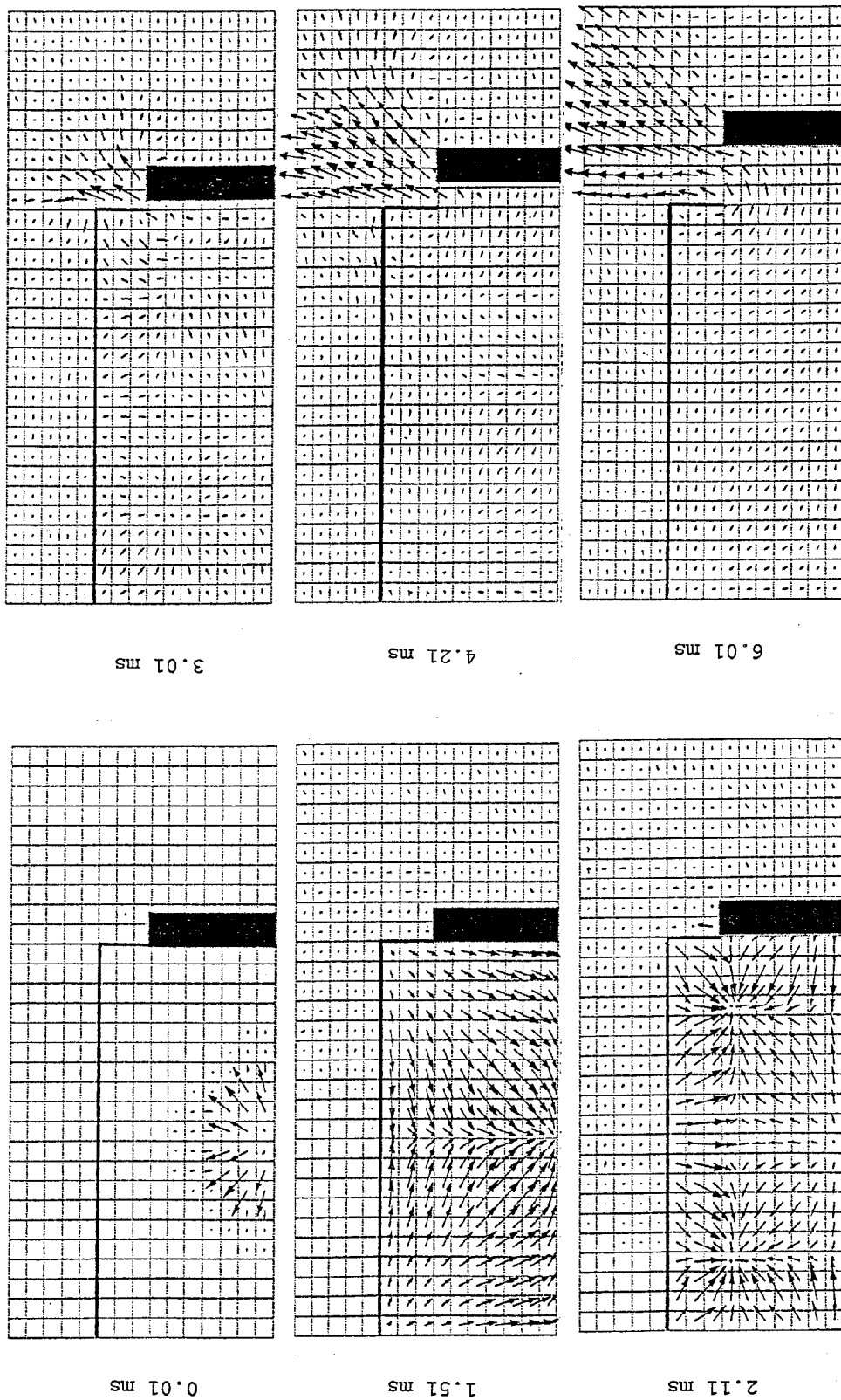


FIGURE 6 : VELOCITY VECTOR PLOTS AT SELECTED TIMES (CASE 3)



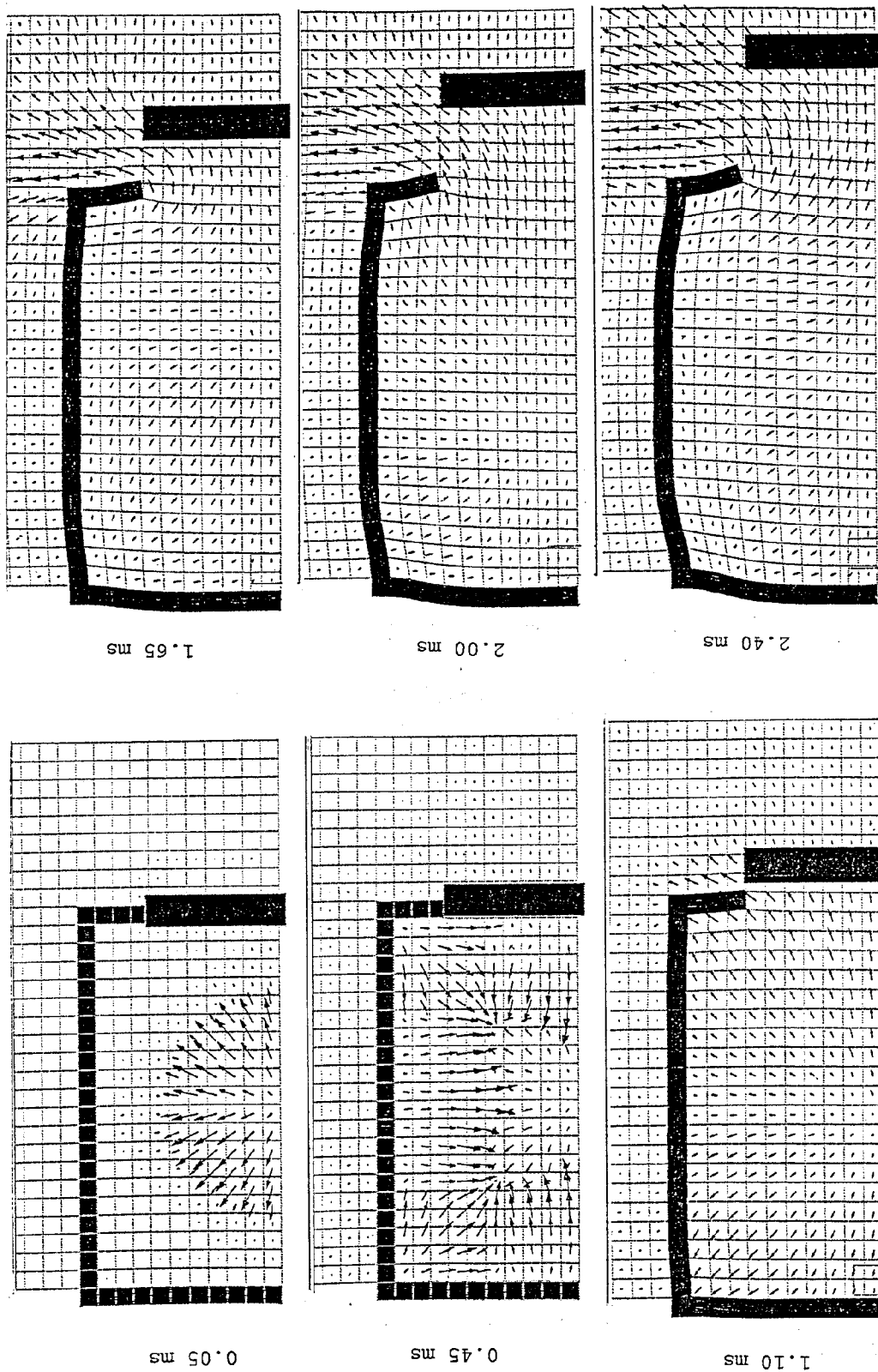


FIGURE 7 : VELOCITY VECTOR PLOTS AT SELECTED TIMES (CASE 4)

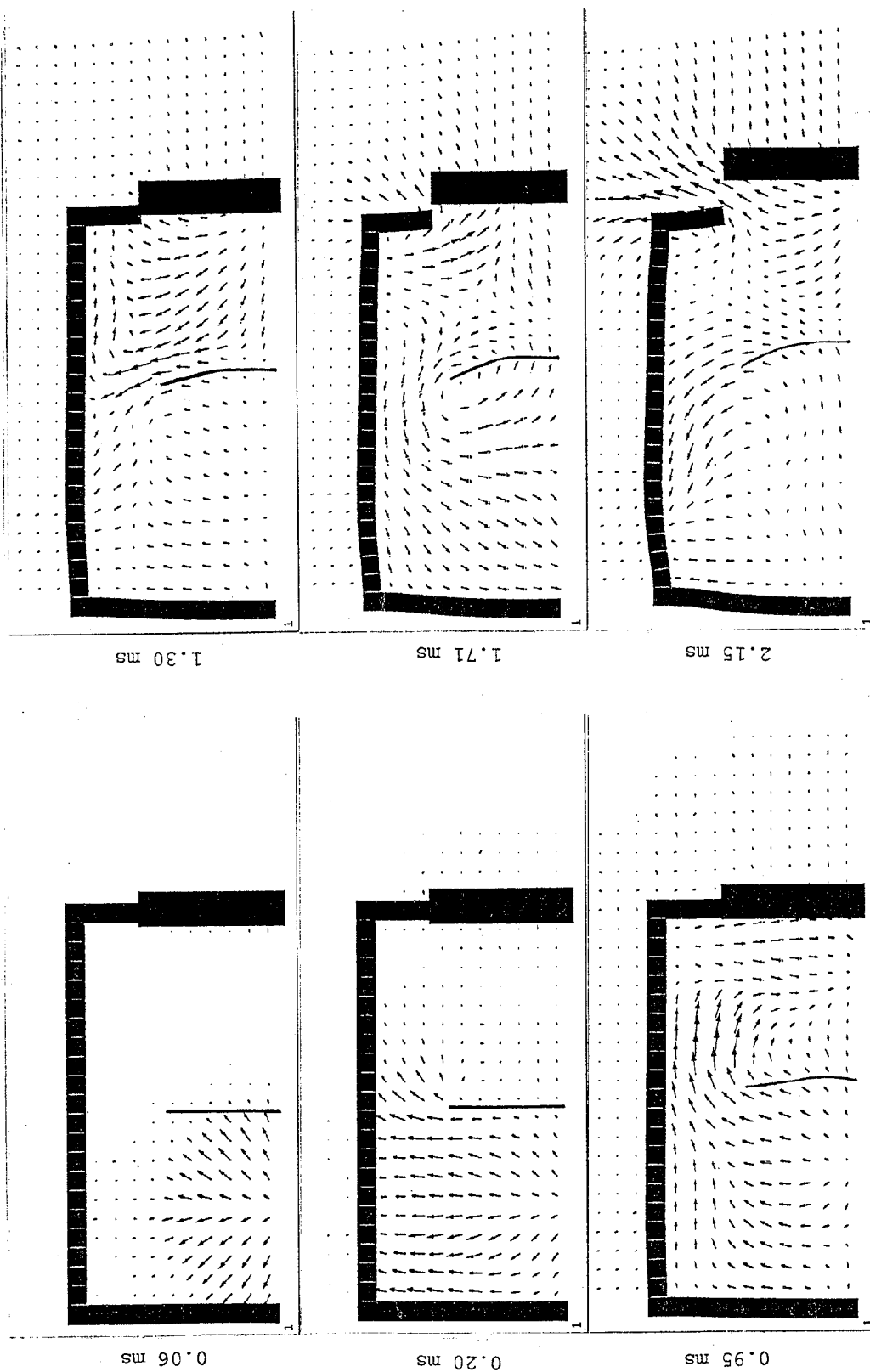


FIGURE 8 : VELOCITY VECTOR PLOTS AT SELECTED TIMES (CASE 5)

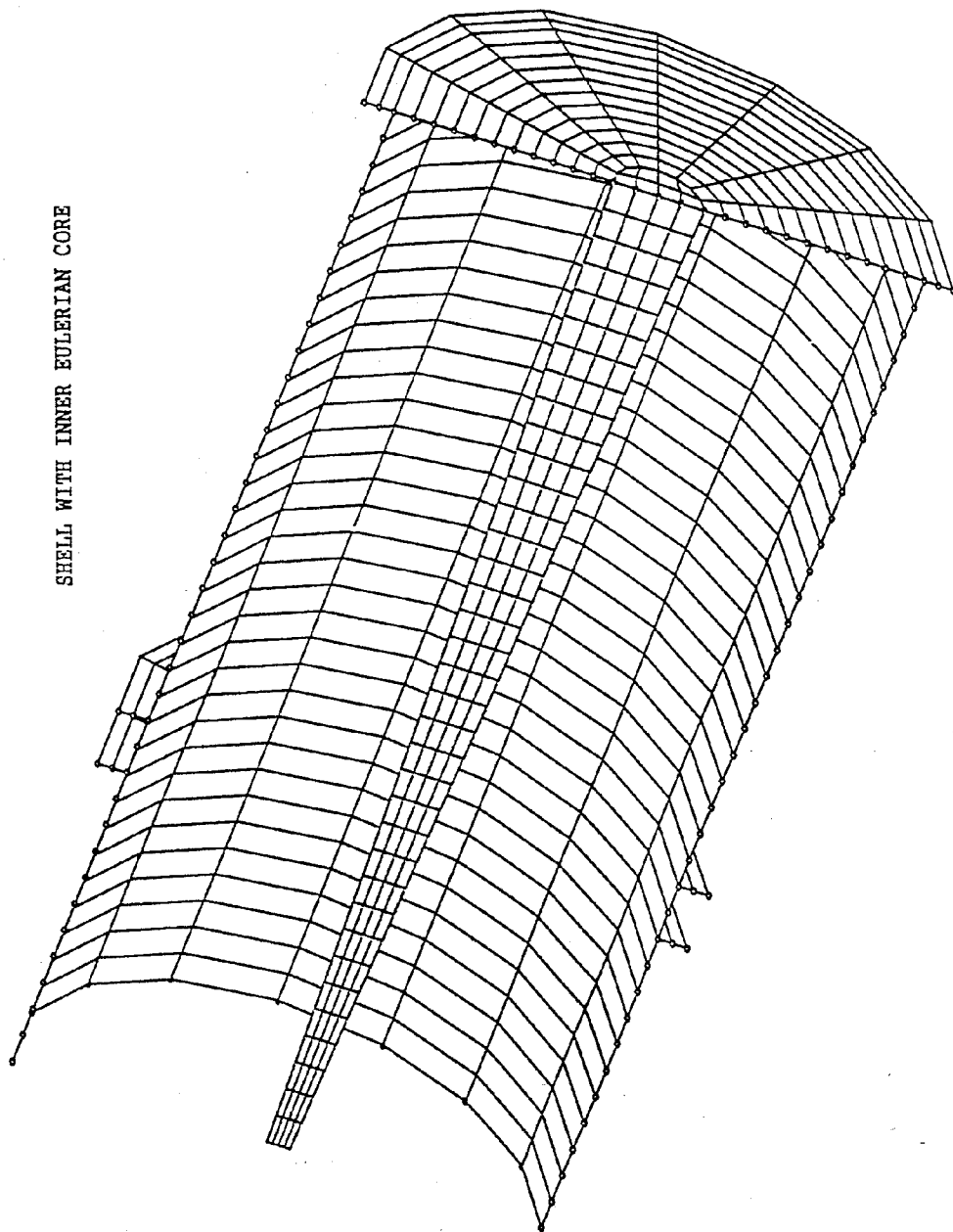


FIGURE 9 : COMPUTATIONAL MESH FOR THE CYLINDRICAL CONTAINER.  
(THE EULERIAN ELEMENTS ARE NOT SHOWN,  
EXCEPT FOR THE CORE NEAR THE SYMMETRY AXIS).

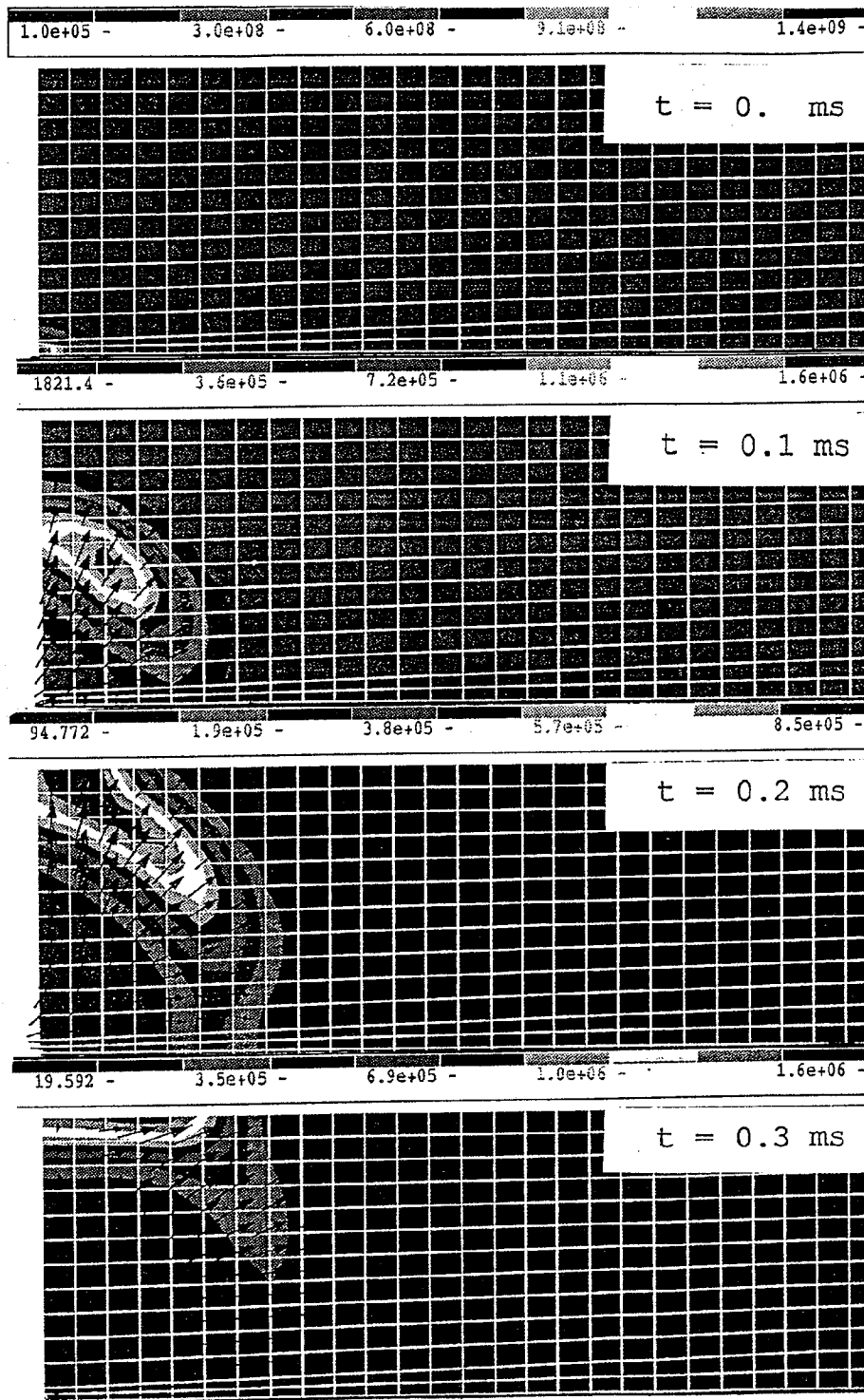


FIGURE 10 : VELOCITY VECTOR PLOTS AT SELECTED TIMES (CASE 6)

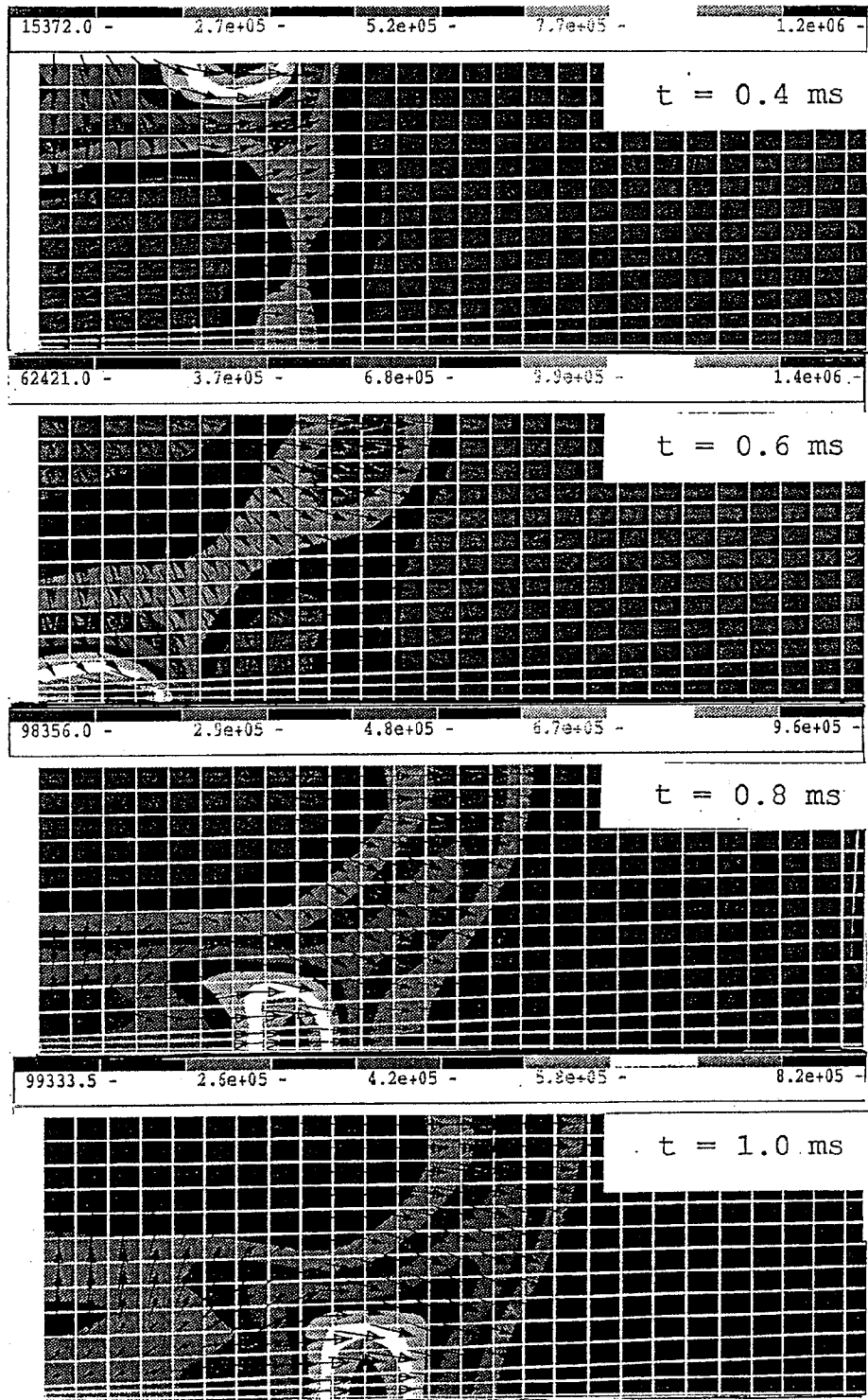


FIGURE 11 : VELOCITY VECTOR PLOTS AT SELECTED TIMES, CONTINUED, (CASE 6)

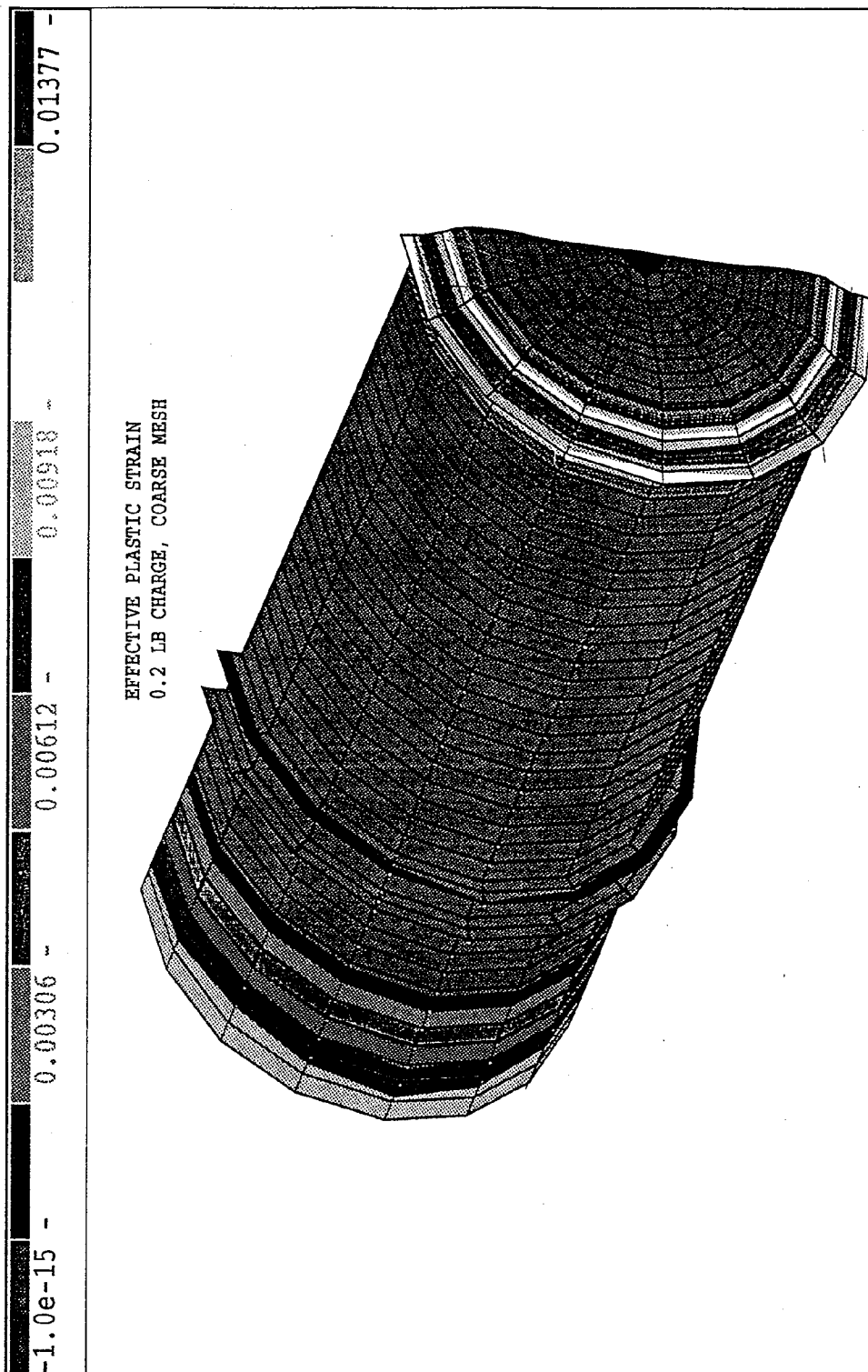


FIGURE 12 : CONTOURS OF EFFECTIVE PLASTIC STRAIN.  
(0.2 LB. CHARGE, 0.003 STRAIN AT ELASTIC LIMIT).